Synthesis, Structure, Magnetism, and Spectroscopic Properties of Some Mono- and Dinuclear Nickel Complexes Containing Noninnocent Pentane-2,4-dione Bis(*S*-alkylisothiosemicarbazonate)-Derived Ligands

Vladimir Arion,*[1a,d] Karl Wieghardt,*[1a] Thomas Weyhermueller,[1a] Eckhard Bill,[1a] Vukadin Leovac,[1b] and Anna Rufinska[1c]

Max-Planck-Institut für Strahlenchemie, Stiftstrasse 34-36, D-45470 Mülheim an der Ruhr, Germany, Institute of Chemistry, Faculty of Sciences, University of Novi Sad, Trg. D. Obradovica 3, 21000 Novi Sad, Yugoslavia, and Max-Planck-Institut für Kohlenforschung, Kaiser-Wilhelm-Platz, 1, D-45470 Mülheim an der Ruhr, Germany

Received July 10, 1996[⊗]

Deprotonation of $[Ni^{II}(H_2L^1)]I\cdot 0.5CH_3OH$ **(1)**, where $(H_2L^1)^-$ represents the ligand pentane-2,4-dione bis(*S*-methylisothiosemicarbazonate(−), in an ethanol solution of aqueous ammonia under argon affords air-sensitive red-brown $[Ni^{II}(HL^1)]\cdot C_2H_5OH$ **(2)**. Air oxidation of **2** in ethanol/NH_3 yields the paramagnetic green-black dinuclear species $[Ni(L^1-L^1)Ni]$ **(3)** where the ligand $(L^1-L^1)^{6-}$ is formed by oxidative C−C coupling at the methine carbon atoms of $(L^1)^{3-}$. In this formulation the nickel ions are trivalent. Reaction of **3** in ethanol with concentrated HCl affords red diamagnetic $[Ni^{II}(H_2L^1-L^1H_2)Ni1I^I]Cl_2\cdot 0.5C_2H_5OH$ **(4)**. This reaction is a 2 electron reduction of **3** with concomittant protonation at the ligand. Deprotonation of **4** in C_2H_5OH/ammonia under argon gives red-brown $[Ni^{II}(HL^1-L^1H)Ni^{II}]\cdot C_2H_5OH$ **(5)**. Replacement of the *S*-methyl groups in $(H_2L^1)^-$ by two dodecyl groups, $(CH_2)_{11}CH_3$, gives the ligand $(H_2L^2)^-$; the complexes $[Ni^{II}(H_2L^2)I$ **(6)** and their dinuclear, oxidized forms $[Ni(L^2-L^2)Ni]$ **(7)** have been prepared analogously. The molecular structure of **3** ($C_{18}H_{28}N_{12}Ni_2S_4$) has been determined by X-ray crystallography. Crystal data for **3**: space group $P\bar{1}$ with $a = 11.475(2)$ Å, $b = 13.615(1)$ Å, $c = 18.207(6)$ Å, $\alpha = 83.87(1)°$, $\beta = 88.36(1)°$, $\gamma = 72.58(1)°$, $V = 2698.7(10)$ Å^3, and $Z = 2$. The structure refinement converged to $R = 0.066$ for 8865 unique reflections. Electronic and NMR spectra, the magnetism, and electrochemistry of new compounds are reported. It is shown that 3,4-diacetyl-2,5-hexanedione-tetrakis(*S*-alkylisothiosemicarbazonates) are noninnocent ligands in **3** and **7**.

Introduction

It is well established that the template condensation reaction between pentane-2,4-dione (Hacac) and *S*-alkylisothiosemicarbazide hydroiodide[2] (1:2) in methanol or ethanol in the presence of a divalent metal ion produces complexes containing the ligand pentane-2,4-dionebis(*S*-alkylisothiosemicarbazone) as is depicted in Scheme 1.[3] This ligand possesses a rather complicated coordination behavior toward redox-active and inactive transition metal ions because it can exist (i) in various protonated forms such as $(LH_3)^0$, $(LH_2)^-$, $(LH)^{2-}$, and $(L)^{3-}$ (Scheme 1)[3] and (ii) it can be oxidized by two electrons where again two different protonated forms have been identified $(HL)^0$ and $(L)^-$.[4] Note that $(L)^{3-}$ is formally a 14 π-electron and $(L)^-$ is a 12 π-electron system. Thus, the ligand which binds via four nitrogen atoms in a equatorial plane of a given coordination polyhedron (square planar, square-based pyramidal, octahedral), belongs to the interesting class of noninnocent[5] ligands. This has recently been demonstrated by the reaction of the square-based pyramidal complex $[Fe^{IV}(L)I]$ with cyanide, which gives reversibly the octahedral iron(II) species $[Fe^{II}(L)(CN)_2]^-$ (formally a reductive addition reaction).[4]

Furthermore, it has recently been discovered[6] that oxidative C−C coupling of two coordinated $(LH)^{2-}$ ligands constitutes a new viable reaction path in this chemistry. Thus, the mononuclear nickel(II) complex $[Ni^{II}(H_2L^1)]I\cdot 0.5CH_3OH$[7] or $[Ni^{II}(H_2L^1)]I$[3a] (the structure of which is schematically displayed in Figure 1) was shown to react in an ethanol/NH_3 mixture with dioxygen or iodine with formation of green-black crystals of a

⊗ Abstract published in *Advance ACS Abstracts,* January 1, 1997.

(1) (a) Max-Planck-Institut für Strahlenchemie. (b) University of Novi Sad. (c) Max-Planck-Institut für Kohlenforschung. (d) On sabbatical leave of absence from the Institute of Chemistry, Moldova Academy of Sciences, 2028 Chishinau, Moldova.

(2) Freund, M.; Paradies, Th. *Ber. Dtsch. Chem. Ges.* **1901**, *34*, 3110.

(3) Structurally characterized examples. (a) $[Ni^{II}(^{Me}LH_2)]I$: Simonov, Yu. A.; Belsky, V. K.; Gerbeleu, N. V.; Shova, S. G.; Arion, V. B. *Dokl. Akad. Nauk SSSR* **1985**, *282*, 620. (b) $[Ni^{II}(^{Et}LH_2)]I\cdot {}^2/_3H_2O\cdot {}^1/_3C_2H_5OH$: Simonov, Yu. A.; Gradinaru, J. I.; Dvorkin, A. A.; Bourosh, P. N.; Gerbeleu, N. V. *Koord. Khim.* **1995**, *21*, 214. (c) $[Co^{III}(^{Me}LH_2)I]I\cdot CH_3OH$: Arion, V. B.; Simonov, Yu. A.; Gerbeleu, N. V.; Dvorkin, A. A.; Gradinaru, J. I.; Malinowsky, T. I. *Dokl. Acad. Nauk SSSR* **1992**, *325*, 502. (d) $[Fe(NO)(^{Me}LH)]NO_3$: Gerbeleu, N. V.; Arion, V. B.; Simonov, Yu. A.; Zavodnik, V. E.; Stavrov, S. S.; Turta, K. I.; Gradinaru, J. I.; Birca, M. S.; Pasynskii, A. A.; Ellert, O. G. *Inorg. Chim. Acta* **1992**, *202*, 173. (e) $[\{Fe^{IV}(^{Me}L)\}_2(\mu\text{-}O)]$: Leovac, V. M.; Herak, R.; Prelesnik, B.; Niketic, S. R. *J. Chem. Soc., Dalton Trans.* **1991**, 2295. (f) $[Fe^{IV}(^{Et}L)I]$: Gerbeleu, N. V.; Simonov, Yu. A.; Arion, V. B.; Leovac, V. M.; Turta, K. I.; Indrichan, K. M.; Gradinaru, J. I.; Zavodnik, V. E.; Malinowsky, T. I. *Inorg. Chem.* **1992**, *31*, 3264. (g) $[Fe^{IV}(^{Me}L)I]$: Knof, U.; Weyhermüller, T.; Wolter, T.; Wieghardt, K.; Bill, E.; Butzlaff, C.; Trautwein, A. X. *Angew. Chem., Int. Ed. Engl.* **1993**, *32*, 1635.

(4) Structurally characterized examples. The complex $[AsPh_4][Fe^{II}(^{Me}L)(CN)_2]CH_2Cl_2\cdot H_2O$ has been described in the paper which reports the structure of $[Fe^{IV}(^{Me}L)I]$: Knof, U.; Weyhermüller, T.; Wolter, T.; Wieghardt, K.; Bill, E.; Butzlaff, C.; Trautwein, A. X. *Angew. Chem., Int. Ed. Engl.* **1993**, *32*, 1635.

(5) Jörgensen, C. K. *Struct. Bonding* **1966**, *1*, 234.

(6) Arion, V. B.; Gerbeleu, N. V.; Levitsky, V. G.; Simonov, Yu. A.; Dvorkin, A. A.; Bourosh, P. N. *J. Chem. Soc., Dalton Trans.* **1994**, 1913−1916.

(7) Gerbeleu, N. V.; Arion, V. B.; Indrichan, K. M. *Zh. Neorg. Khim.* **1985**, *30*, 2833−2837.

S0020-1669(96)00802-6 CCC: $14.00

Scheme 1. Protonation Scheme for the 14 π-Electron System $(^{R}L)^{3-}$ and Its Oxidized 12 π-Electron System $(^{R}L)^{-}$ [a]

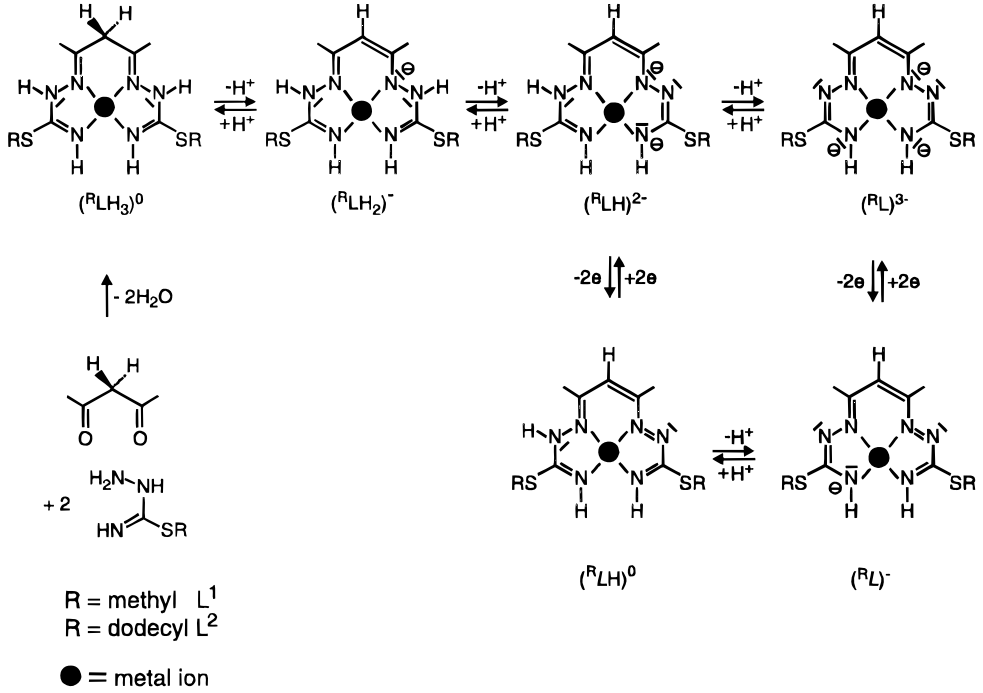

[a] R denotes *S*-methyl of or *S*-dodecyl groups.

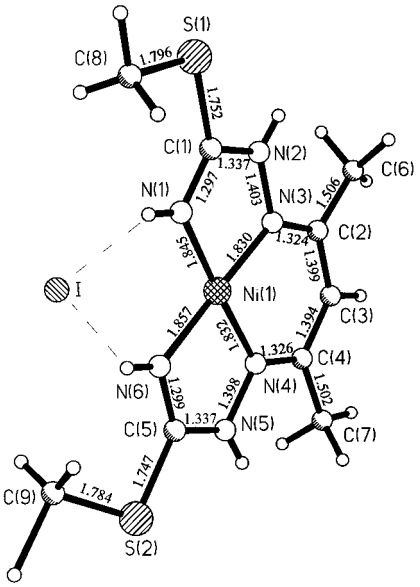

Figure 1. Schematic representation of the molecule $[Ni^{II}(H_2L^1)]I$ in crystals of **1**.

dinuclear species which was formulated as shown below:

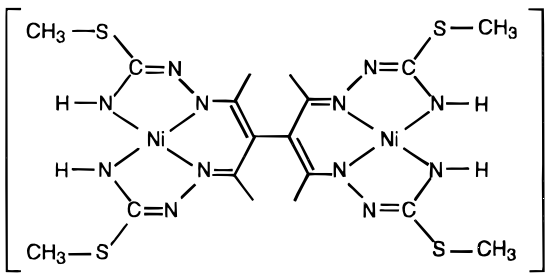

3

At the time[6] it had not been explicitly recognized that in this formulation the ligand is a hexaanion and that—if this is the case—the nickel ions must possess the formal oxidation state +III. Structurally characterized genuine square-planar nickel(III) complexes are quite rare.[8] They are paramagnetic (low-spin d^7). Here we give a detailed report on the structure and spectroscopic properties of the above complex. We will show that the dinucleating ligand $(L^1-L^1)^{6-}$ is noninnocent and that oxidation of 2 equiv of $[Ni^{II}(H_2L^1)]I\cdot 0.5CH_3OH$ **(1)** to the green-black dinuclear species is a *4* electron process and not a simple C−C coupling (*2e* process).

Experimental Section

Abbreviations. The following ligand abbreviations used throughout this work: H_3L^1, pentane-2,4-dione bis(*S*-methylisothiosemicarbazone); H_3L^2, pentane-2,4-dione bis(*S*-dodecylisothiosemicarbazone). The deprotonated ligand forms are designated as shown in Scheme 1. $H_3L^1-L^1H_3$ and $H_3L^2-L^2H_3$ represent the methine carbon atom of $(H_2L^1)^-$ and $(H_2L^2)^-$ C−C coupled ligands 3,4-diacetyl-2,5-hexanedione tetrakis(*S*-methylisothiosemicarbazonate) and its dodecyl derivative; Hacac, pentane-2,4-dione; DMSO, dimethyl sulfoxide. We will designate the 2e oxidized forms of $(L)^{3-}$ by italics $(L)^{-}$.

Synthesis of Complexes. $[Ni^{II}(H_2L^1)]I\cdot 0.5CH_3OH$ (1).[7] A mixture of $Ni(CH_3COO)_2\cdot 4H_2O$ (2.5 g, 10.0 mmol), *S*-methylisothiosemicarbazide hydroiodide[2] (4.66 g, 20.0 mmol), and Hacac (1.5 g, 15.0 mmol) in methanol (40 mL) was heated under reflux for 10 min and allowed to stand at ambient temperature. Gold-brown needlelike crystals were collected by filtration, washed with methanol and ether, and dried in air. Yield 2.5 g (53%). Recrystallization of this product from dry ethanol gives unsolvated $[Ni^{II}(H_2L^1)]I$: ^{1}H NMR δ (DMSO-d_6) 11.64 (s, 2H, NNH), 7.44 (s, 2H, NH), 5.05 (s, 1H, − CH═), 2.63 (s, 6H, SCH_3), 2.31 (s, 6H, CH_3); ^{13}C NMR δ (DMSO-d_6) 157.23 ($C_{tert}S$), 145.58 (C_{tert}), 93.41 (CH═), 19.28 (CH_3), 13.48 (SCH_3); the assignment was proven by 2D-NMR spectra (^{1}H, ^{1}H and ^{1}H, ^{13}C via long-range couplings); electron impact (EI) mass spectrum *m/z* 330 ($[M - HI]^+$).

$[Ni^{II}(HL^1)]\cdot C_2H_5OH$ (2). To a solution of **1** (1.0 g; 2.1 mmol) in ethanol (25 mL) under an argon blanketing atmosphere was added an aqueous concentrated ammonia solution (2 mL). Red-brown microcrystals of **2** precipitated which were collected by filtration, washed with dry ethanol, and dried under argon. The material is air-sensitive. Yield 0.5 g (63%). Anal. Calcd for $C_{11}H_{22}N_6NiOS_2$ (fw = 377.1):

(8) (24) Collins, T. J.; Nichols, T. R.; Uffelman, E. S. *J. Am. Chem. Soc.* **1991**, *113*, 4708−4709.

C, 35.03; H, 5.87; N, 22.28; S, 17.00. Found: C, 34.6; H, 5.7; N, 21.7; S, 17.7. ^{1}H NMR δ (DMSO-d_6) 10.70 (br s, 1H, NNH), 6.10 (br s, 2H, NH), 4.84 (s, 1H, CH═), 4.35 (br s, 1H, OH), 3.45 (q, 2H, CH_2), 2.49 (s, 6H, SCH_3), 2.20 (s, 6H, CH_3), 1.06 (t, 3H, CH_3); ^{13}C NMR δ (DMSO-d_6) 154.78 ($C_{tert}S$), 143.07 (C_{tert}), 92.29 (CH═), 56.02 (CH_2, EtOH), 19.53 (CH_3), 18.53 (CH_3, EtOH), 14.04 (SCH_3); electron impact (EI) mass spectrum *m/z* 330 ([M]$^+$).

[Ni(L^1−L^1)Ni] (3). An aqueous concentrated ammonia solution (3.5 mL) was added to a solution of **1** (1.4 g; 2.9 mmol) in ethanol (80 mL) at 60−70 °C. The filtered red solution was allowed to stand at ambient temperature in an open vessel in the presence of air for 24 h after which time a dark green precipitate had formed. Recrystallization from CH_2Cl_2 (250 mL) saturated with *n*-pentane produced green-black crystals of **3** which were suitable for X-ray crystallography. Yield 0.68 g (70%). Anal. Calcd for **3**, $C_{18}H_{28}N_{12}Ni_2S_4$ (fw = 658.1): C, 32.85; H, 4.29; N, 25.54. Found: C, 32.5; H, 4.3; N, 25.2. Fast atom bombardment (FAB) mass spectrum *m/z* 658 ([M + 2H]$^+$).

[Ni^{II}(H$_2$L^1−L^{1}H$_2$)Ni^{II}]Cl$_2$·0.5C$_2$H$_5$OH (4). Concentrated hydrochloric acid (0.3 mL) in ethanol (20 mL) was added dropwise at ambient temperature to an ethanol solution (50 mL) of **3** (0.5 g; 0.76 mmol). A color change from green to red was observed. After the reaction volume was reduced to ∼$^1/_3$ under reduced pressure, red microcrystals precipitated which were collected by filtration, washed with ethanol, and air-dried. Yield 0.15 g (26%). Anal. Calcd for $C_{19}H_{35}Cl_2N_{12}Ni_2O_{0.5}S_4$ (fw = 756.1): C, 30.18; H, 4.67; N, 22.23; Cl, 9.38. Found: C, 29.7; H, 4.4; N, 22.6; Cl, 9.7. ^{1}H NMR δ (DMSO-d_6) 11.65 (br s, 4H, NNH), 8.50 (s, 4H, NH), 3.8−3.4 (br s, 0.5H, OH), 3.42 (q, 1H, CH_2), 2.66 (s, 12H, SCH_3), 1.97 (s, 12H, CH_3), 1.04 (t, 1.5H, CH_3); ^{13}C NMR δ (DMSO-d_6) 156.97 ($C_{tert}S$), 147.26 (C_{tert}), 102.41 (γ-C), 55.97 (CH_2, EtOH), 18.14 (CH_3), 18.52 (CH_3, EtOH), 13.79 (SCH_3); electrospray ionization (ESI) mass spectrum *m/z* 330 ([M − 2Cl]$^{2+}$).

[Ni^{II}(HL^1−L^{1}H)Ni^{II}]·C$_2$H$_5$OH (5). Complex **4** (0.55 g, 0.73 mmol) was deprotonated in an ethanol solution (8 mL) under an argon blanketing atmosphere with aqueous concentrated ammonia (1.0 mL). A red-brown microcrystalline precipitate formed which was collected by filtration, washed with deoxygenated ethanol, and dried under argon. This material is very air-sensitive. Yield 0.15 g (29%). Anal. Calcd for $C_{20}H_{36}N_{12}Ni_2OS_4$ (fw = 706.2): C, 34.01; H, 5.14; N, 23.80. Found: C, 34.4; H, 4.8; N, 23.7. ^{1}H NMR δ (DMSO-d_6) 11.04 (br s, 2H, NNH), 6.40 (br s, 4H, NH), 4.33 (br s, 1H, OH), 3.42 (q, 2H, CH_2), 2.49 (s, 12H, SCH_3), 1.98 (s, 12H, CH_3), 1.04 (t, 3H, CH_3).

[Ni^{II}(H$_2$L^2)I (6). To a solution of $Ni(CH_3COO)_2$·$4H_2O$ (1.25 g, 5.0 mmol) in ethanol (15 mL) were added *S*-dodecylisothiosemicarbazide hydroiodide (3.87 g, 10.0 mmol) in ethanol (15 mL) and Hacac (0.5 g, 5.0 mmol). This solution was heated under reflux for 10 min and allowed to stand at ambient temperature. Brown crystals were collected by filtration, washed with ethanol and ether, and dried in air. Yield 2.2 g (57%). Anal. Calcd for $C_{31}H_{61}N_6NiIS_2$ (fw = 767.6): C, 48.51; H, 8.01; N, 10.95. Found: C, 48.2; H, 8.0; N, 10.9. ^{1}H NMR δ (DMSO-d_6) 11.66 (s, 2H, NNH), 7.57 (s, 2H, NH), 5.08 (s, 1H, CH═), 3.18 (t, 4H, SCH_2), 2.25 (s, 6H, CH_3), 1.63 (m, 4H, CH_2), 1.21 (br s, 36H, CH_2), 0.83 (t, 6H, CH_3). The solution of *S*-dodecylisothiosemicarbazide hydroiodide in ethanol was obtained by heating a mixture of thiosemicarbazide (0.91 g, 10.0 mmol) and dodecyl iodide (2.96 g, 10.0 mmol) in dry ethanol (15 mL) until complete dissolution of the reactants was observed.

[Ni(L^2-L^2)Ni] (7). To a warm ethanol solution (40 mL) of **6** (1.4 g, 1.8 mmol) was added an aqueous concentrated ammonia solution (1.8 mL). After filtration, the red solution was allowed to stand in an open vessel in the presence of air of 24 h during which time a green-black microcrystalline precipitate formed which was recrystallized from acetone. Yield 0.85 g (73%). Anal. Calcd for $C_{62}H_{116}N_{12}Ni_2S_4$ (fw = 1275.3): C, 58.39; H, 9.17; N, 13.8; S, 10.06. Found: C, 58.0; H, 9.0; N, 12.9; S, 10.4. ESI mass spectrum *m/z* 1272 ([M]$^+$).

Physical Measurements. Infrared spectra were recorded on a Perkin-Elmer 2000FT-IR as KBr disks (4000−400 cm^{-1}). Magnetic susceptibility measurements of well-ground solid samples were performed on a SQUID magnetometer (Quantum Design Model MPMS). Diamagnetic corrections were made by use of tabulated Pascal's constants. Fast atom bombardment mass spectra of solid samples in a *o*-nitrobenzaldehyde matrix were obtained by using Varian MAT 311A and Varian MAT 95 spectrometers. Solution ^{1}H and ^{13}C NMR spectra were recorded on a Bruker AC 270 and AM 400 spectrometer operating at 270 and 400 MHz, respectively. Chemical shifts for ^{1}H and ^{13}C NMR spectra were referenced to residual ^{1}H and ^{13}C present in deuterated solvents. Solid state CP/MAS ^{13}C NMR spectra were measured on a Bruker MSL-300 spectrometer equiped with CP/MAS double-bearing probe and a Bruker BV-1000 temperature control unit. ZrO_2 rotors (7 mm o.d.) completely or partially filled (when necessary under argon) were spun at spin rates of 4 kHz. External standards were adamantane for ^{13}C CP/MAS spectra, δ_{TMS} (CH_2) 38.40. A typical 90° pulse for ^{1}H was ∼4 μs. Absorption spectra were recorded on a Perkin-Elmer Lambda 19 spectrophotometer. Cyclic voltammetric measurements were performed using an EG&G Model 273A potentiostat. A three-electrode cell was used consisting of a glassy carbon working electrode, a platinum counter electrode, and a Ag/AgCl/saturated LiCl(EtOH) reference electrode. Ferrocene was used as internal standard. Deaeration of all solutions was accomplished by passing a stream of high-purity argon through the solution for 10 min prior to the measurements and then maintaining a blanketing atmosphere of argon over the solution during the measurements.

Table 1. Crystallographic Data for **3**

formula	$C_{18}H_{28}Ni_2N_{12}S_4$	*Z*	4
fw	658.1	space group	$P\bar{1}$
a, Å	11.475(2)	*T*, °C	20
b, Å	13.615(1)	λ, Å	0.710 69
c, Å	18.207(6)	ρ_{calc}, g cm^{-3}	1.62
α, deg	83.87(1)	μ, cm^{-1}	17.33
β, deg	88.36(1)	R^a	0.066
γ, deg	72.58(1)	$R_w{}^b$	0.188

^{a} $R = \sum(|F_o| - |F_c|)/\sum(|F_o|)$. ^{b} $R_w = [\sum w(|F_o|^2 - |F_c|^2)^2/\sum(|F_o^2|)^2]^{1/2}$; $w = 1/[\sigma^2(F_o^2) + 0.105P + 7.400P]$, where $P = (F_o^2 + 2F_c^2)/3$.

Crystal Structure Determination. X-ray diffraction measurements were performed on a Enraf-Nonius CAD4 diffractometer, using graphite-monochromated Mo Kα radiation. Crystal data and data collection parameters are given in Table 1. Intensities were measured in the $\omega/2\theta$ scan mode and were corrected for decay of three control reflections (less than 5%), controlled every hour and for Lorentz and polarization effects. An empirical absorption correction (ψ scan) was applied (transmission, minimum 0.911; maximum 1.000). The nickel atoms were located by conventional Patterson synthesis, and the remaining non-hydrogen atoms were located by successive difference Fourier syntheses. Some of the imine H atoms were located in the final difference Fourier synthesis; all others were placed at calculated positions. Two of the eight terminal thiomethyl groups are disordered. The final difference map has relatively high residual peaks and holes (of the order +2.4 to −2.7 e Å^3) associated with the disorder in molecule **3B** which was not resolved. Although it is possible to split atoms C24 and C33 (but not S8), this did not improve the final *R* value or diminish the estimated standard deviations, and therefore, we did not use the split atom model. Attempts to obtain a low-temperature data set failed as the crystal shattered upon cooling.

The function minimized during full-matrix least-squares refinement was $\sum w\{|F_o| - |F_c|\}^2$. Details of the computer programs used are given in ref 9. Neutral-atom scattering factors and anomalous dispersion corrections for non-hydrogen atoms were taken from ref 10. For further details of the crystal structure determination and final atomic coordinates and equivalent isotropic thermal parameters, see Supporting Information.

Results

Synthesis and Characterization of Complexes. Scheme 2 summarizes the synthetic routes to new complexes. The

(9) Computer programs used. Data reduction: DATAP, Coppens, P.; Leiserowitz, L.; Rabinovich, D. *Acta Crystallogr*. **1965**, *18*, 1035. Structure solution: SHELXS-86, Sheldrick, G. M. *Acta Crystallogr*. **1990**, *A46*, 467. Structure refinement: Sheldrick, G. M. SHELXL-93, Program for crystal structure refinement, University of Göttingen, Göttingen, Germany, 1993. Molecular diagrams: ORTEP, Johnson, C. K. Report ORNL-5138, Oak Ridge National Laboratory, Oak Ridge, TN, 1976. Computer: Alpha 3000-700.

(10) Scattering factors: *International Tables for X-ray Crystallography*; Kluwer Academic Press: Dordrecht, The Netherlands, 1992; Vol. C, Tables 4.2.6.8 and 6.1.1.4.

Scheme 2. Syntheses of Complexes

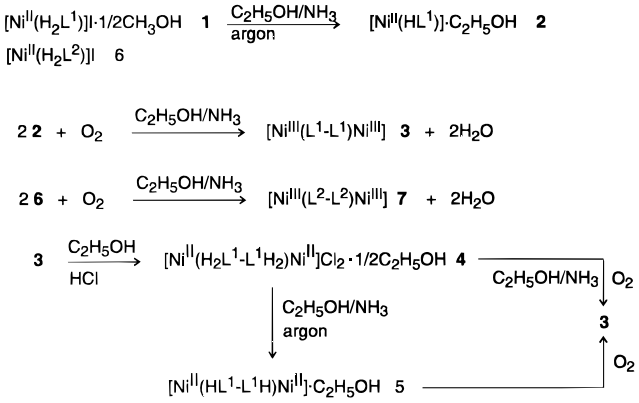

template reaction of $Ni(CH_3COO)_2 \cdot 4H_2O$ with pentane-2,4-dione, *S*-alkylisothiosemicarbazide hydroiodide[2] (1:1:2) in methanol produces in good yields the red complex $[Ni^{II}(H_2L^1)]I \cdot 0.5CH_3OH$ **(1)**.[7] The structure of $[Ni^{II}(H_2L^1)]I$[3a] obtained by recrystallization of **1** is shown in Figure 1. The diamagnetic complex consists of a square-planar nickel(II) ion coordinated to two imine (N1, N6) and two hydrazine (N3, N4) nitrogens of the monoanionic ligand pentane-2,4-dione bis(*S*-methylisothiosemicarbazidate). Two hydrazine nitrogens N2 and N5 are protonated. The uncoordinated iodide forms four intermolecular hydrogen bonding contacts to the hydrazine and imine protons.

Deprotonation of one of these hydrazine protons in **1** is readily achieved in an ethanol solution of **1** in the absence of oxygen by addition of an aqueous solution of ammonia. Red-brown microcrystals of diamagnetic $[Ni^{II}(HL^1)] \cdot C_2H_5OH$ **(2)** precipitate. This material is very sensitive to oxygen both in the solid state and in solution. The solution ^1H NMR spectrum of **2** in DMSO exhibits two broad signals at $\delta = 10.70$ and 6.10 ppm, (intensity ratio is 1:2) which are assigned to one hydrazine proton (at N2 or N5) and two imine protons (N1, N6), respectively. Atom labeling is as in Figure 1. We propose the following structure for **2**:

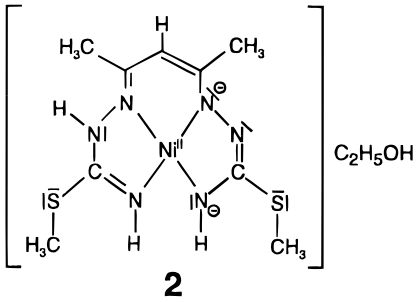

2

The two halves of the coordinated ligand $(HL^1)^{2-}$ are not symmetric due to the protonation of only one hydrazine nitrogen atom.

When the above ethanolic solution of **1**, to which ammonia had been added, was allowed to stand in an open vessel in the presence of air, a change of color from red to green was observed. Green-black microcrystals of $[Ni(L^1-L^1)Ni]$ **(3)** precipitated from such solutions.[6] The amount of dioxygen consumed during the reaction was determined manometrically. It was found that per 2 equiv of **1** 1 equiv of O_2 was consumed

$$2\mathbf{1} + O_2 \rightarrow \mathbf{3} + 2H_2O \qquad (1)$$

The same product **3** was quantitatively obtained when iodine was used as oxidant under an argon atmosphere instead of dioxygen

$$2\mathbf{1} + 2I_2 \rightarrow \mathbf{3} + 4HI \qquad (2)$$

The product **3** consists of a dinuclear neutral species $[Ni(L^1-L^1)Ni]$ as was determined by X-ray crystallography (see below). Oxidative C−C coupling at the methine carbon atoms of the ligand has taken place. This is formally a 2 electron oxidation

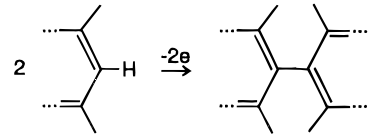

(3)

As the stoichiometry of reactions 1 and 2 clearly shows that per 2 equiv of **1** *4* electrons are released a further 2 electron oxidation of the ligand or a metal-centered oxidation of the two Ni^{II} to Ni^{III} must have occurred. The original formulation of **3** shown in the Introduction implies the presence of two trivalent Ni^{III} ions and a hexaanionic ligand $(L^1-L^1)^{6-}$.

Complex **3** is paramagnetic both in solution and in the solid state at room temperature (see below). The solid state structure of **3** and its electronic structure are extremely interesting. We will show that the ligand is noninnocent, and the description of **3** as a dinuclear Ni_2 complex with a localized +III oxidation state at the metal ions is not appropriate.

When an ethanol solution of **3** was acidified with concentrated HCl (or CF_3SO_3H), a color change from green to red was observed and red diamagnetic $[Ni^{II}(H_2L^1-L^1H_2)Ni^{II}]Cl_2 \cdot 0.5C_2H_5OH$ **(4)** (or its triflate salt) was obtained. Given the diamagnetism of **4** and the similarity of its UV−visible spectrum with that of **1** (Table 2) we propose the following structure for **4**,

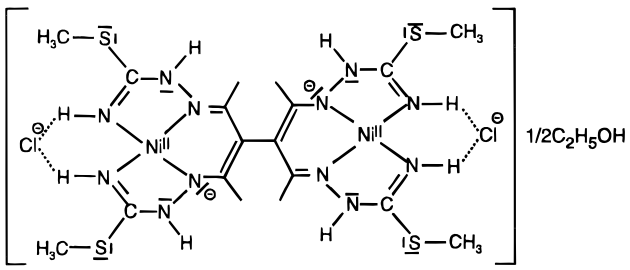

4

which consists of the dianionic ligand $(H_2L^1-L^1H_2)^{2-}$ and two Ni^{II} and two noncovalently bound chloride ions.

The presence of protonated hydrazine nitrogens is clearly detected in the infrared spectrum by two new ν(NH): 2996 and 2920 cm^{-1} bands. The ESI mass spectrum of an ethanol solution of **4** displays a doubly charged molecular ion peak at $m/z = 660/2 = 330$. The spectroscopic properties (UV−visible, ^1H and ^{13}C NMR, IR) of **4** and of its mononuclear analog **1** are very similar. In the ^1H NMR spectra (DMSO-d_6) of **1** and **4**, two signals of equal intensity for NH protons are observed; a downfield shift for NNH protons of hydrazine residues ($\delta =$ 11.64 **(1)**, 11.65 **(4)** ppm) with respect to the imine NH protons ($\delta = 7.44$ **(1)**, 8.50 **(4)** ppm) is observed. Two singlets, one for SCH_3 and another for the methyl groups of the Hacac moieties, are present in the spectrum of **1** and **4**, respectively. This agrees with C_{2v} symmetry of **1** and C_i symmetry of **4**. No methine proton signal is observed in the ^1H NMR spectrum of **4**. This indicates that both halves of the molecule **4** are connected via a simple $C(sp^2)-C(sp^2)$ bond. The solution ^{13}C NMR spectra (DMSO-d_6) of **1** and **4** are also very similar (see Experimental Section); five carbon signals for the ligands are expected and observed, respectively.

From the above data it follows that the reaction of **3** with HCl or (CF_3SO_3H) in ethanol yielding **4** cannot be a simple

Table 2. Electronic Spectra of Complexes

complex	solvent	λ_{max}, nm (ϵ = L mol^{-1} cm^{-1})
1	CH_3OH	509 (184), 390 (1.66×10^4), 375 (1.35×10^4), 285 (1.70×10^4), 262 (1.46×10^4), 219 (3.2×10^4)
2	$(CH_3)_2CO$	658 (1307), 472 (1.08×10^4), 403 (12.44×10^4), 386 (11.63×10^4)
3	$CHCl_3$	821 (9.7×10^3), 657 (1.15×10^4), 489 (1.11×10^4), 403 (2.2×10^4), 338 (2.1×10^4), 312 (2.1×10^4), 275 (3.9×10^4)
4	CH_3OH	506 (520), 405 (2.38×10^4), 389 (1.94×10^4), 298 (4.1×10^4), 248 (3.3×10^4), 215 (3.7×10^4)
7	$CHCl_3$	824 (1.0×10^3), 662 (1.2×10^4), 492 (1.14×10^4), 407 (2.3×10^4), 340 (2.2×10^4), 312 (2.1×10^4), 275 (3.9×10^4)

protonation reaction but is a more complex redox reaction. We have not been able to identify the oxidation product; acetaldehyde or acetic acid appear to be the most likely species

$$\mathbf{3} \xrightarrow[C_2H_5OH]{HCl} \mathbf{4} + \text{unknown oxidation product} \qquad (4)$$

Since **1** is readily deprotonated affording **2**, we have carried out the analogous reaction with **4**. From an ethanol solution of **4**, in the absence of oxygen, to which aqueous ammonia had been added, diamagnetic red-brown microcrystalline [Ni^{II}(HL^1−L^{1}H)Ni^{II}]·C_2H_5OH **(5)** was obtained. We therefore propose the following structure for **5** which contains two square-planar diamagnetic Ni^{II} ions and the ligand (HL^1−L^{1}H)$^{4-}$.

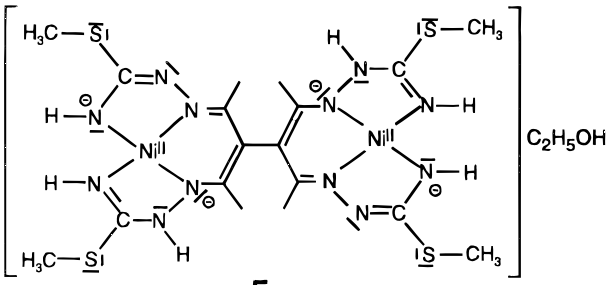

5

The ^{1}H NMR spectrum (see Experimental Section) is in excellent agreement with this proposal. Complex **5** is very air-sensitive: in ethanol solution containing NH_3, complex **3** is rapidly formed in quantitative yield by air oxidation. The stoichiometry is now

$$\mathbf{5} + {}^1/_2O_2 \rightarrow \mathbf{3} + H_2O \qquad (5)$$

Since the magnetic properties of **3** are quite peculiar (see below) and differ in the solid state and in solution considerably, we have synthesized two analogous complexes with sterically more demanding *S*-dodecyl groups instead of the *S*-methyl groups. The mononuclear diamagnetic complex [Ni^{II}(H$_2$L^2)]I **(6)**, which is the exact analog of **1**, has been prepared. It reacts in ethanol/NH_3 solution also with dioxygen affording green-black crystals of [Ni(L^2−L^2)Ni] **(7)**, the analog of **3**. The solubility of **7** in noncoordinating organic solvents is significantly greater than that of **3**. For **7** the positive ion ESI mass spectrum exhibits the molecular ion peak at m/z = 1272 ([M]$^+$). We have also determined the molecular mass of **7** in benzene solution by cryoscopy to be 1070 ± 200 g/mol, which clearly indicates the presence of isolated neutral molecules of [Ni(L^2−L^2)Ni] in solution.

The solution electronic spectra of complexes **1**−**3**, **4**, and **7** are given in Table 3. The spectra of **3** and **4** are displayed in Figure 2. The spectra of **1**, **4**, and **6** are quite similar since they all contain a square-planar Ni^{II} ion in essentially the same ligand environment. The absorption maximum at ∼510 nm is assigned to a $d_{xy} \rightarrow d_{x^2-y^2}$ ($^1A_{2g} \rightarrow {}^1A_{1g}$) transition, which is typical for a Ni^{II}N$_4$ chromorphore. The spectra of **3** and **7** are again similar but very different from those of **1**, **4**, and **6**; both display very intense maxima at ∼820 and ∼660 nm which are not d−d transitions. Simple deprotonation of **1** and **4** yielding **2** and **5** does not produce these spectra.

Crystal Structure of 3. Complex **3** crystallizes in the triclinic space group $P\bar{1}$ and contains two crystallographically independent neutral dinuclear [Ni(L^1−L^1)Ni] molecules per unit cell. Table 3 summarizes important bond distances and angles as well as some intermolecular S···S contacts. Figure 3 shows the structures and atom labels of the two independent molecules **3A** and **3B**.

Each of these two crystallographically independent dinuclear molecules may be considered to be composed of two halves connected by a single C(sp^2)−C(sp^2) bond (C3−C12 in **3A** and C29−C30 in **3B** at 1.507(7) and 1.492(8) Å, respectively). Carbon atoms C3, C12, C29, and C30 are clearly sp^2 hybridized. The dihedral angle between the two mean planes defined by atoms N1, N3, N4, N6, and N7, N9, N10, N12 is 76.8° in **3A** and, analogously, 71.6° in **3B**.

Interestingly, the oxidation of [Ni^{II}(Me$_2$[13]dienatoN$_4$)](ClO$_4$), where Me$_2$[13]dienatoN$_4$ represents the monoanion 11,13-dimethyl-1,4,7,10-tetraaza-10,13-cyclotridecane dienato with iron(III) perchlorate yields a $C_\gamma = C_\gamma$ coupled dinuclear species.[11,12] The methine carbon atoms of the monomer have been oxidatively dehydrogenated and coupled (4e process) via a localized double bond (C−C 1.34(1) Å). In [Ni(CH$_3$CN)-(Me$_2$[13]dienN$_4$)ylidene]$_2^{4+}$ this C−C distance is at 1.37(1) Å (double bond).[12] Oxidation of [Ni^{II}(cyclam)]$^{2+}$ with H_2O_2 produces a dinuclear complex [Ni$_2^{II}$(L^4)](ClO$_4$)$_4$ with a C=C double bond at 1.40(2) Å[13] (cyclam 1,4,8,11-tetraazacyclotetradecane, L^4 = 1,1′-enebicyclo-3,6,10,13-tetraazatetradeca-2,-13-dienylidene).

We have been able to locate the four imine hydrogen atoms in the final difference Fourier map for **3A** but not for **3B**. In no case has residual electron density been detected in the vicinity of any of the uncoordinated hydrazine nitrogen atoms. This suggests to us that the dinucleating ligand in **3** is coordinated in its deprotonated form (L^1−L^1)$^{6-}$.

All nickel ions are coordinated to two imine nitrogens and two hydrazine nitrogens, respectively, in a square-planar fashion. The averaged four Ni−N bond distances in both halves of **3A** are within experimental error identical (average 1.842(5) and 1.850(5) Å) whereas in **3B** they are slightly (not quite significantly) different: at Ni3 an average value of 1.844(5) Å and at Ni4 a value of 1.819(5) Å is found. This may be a structural manifestation of the differing packing of **3A** and **3B** in crystals of **3** (see below). Note that the average Ni−N distances in **1**—a genuine nickel(II) complex—is 1.841(6) Å. In Collins' square-planar localized Ni(III) complex, the average Ni−N distance is also observed at 1.84 Å.[8]

The packing of the neutral molecules **3A** and **3B** in crystals of **3** is rather interesting. Two dinuclear molecules of **3B** form a centrosymmetric pair of dimers via an intermolecular weak stacking interaction between two halves of **3B**. Thus Ni4 and its centrosymmetric counterpart Ni4a form a Ni···Ni interaction at 3.402(2) Å, whereas the atoms Ni3 and Ni3a are not involved

(11) Cunningham, J. A.; Sievers, R. E. *J. Am. Chem. Soc.* **1973**, *95*, 7183.
(12) Mochizuki, K.; Toriumi, K.; Ito, T. *Bull. Chem. Soc. Jpn.* **1984**, *57*, 881.
(13) McAuley, A.; Xu, C. *Inorg. Chem.* **1992**, *31*, 5549.

Table 3. Bond Distances (Å) and Angles (deg) for **3**

Molecule **3A**

Ni(1)−N(1)	1.850(6)	C(10)−N(8)	1.350(7)	N(1)−N(6)	1.828(6)	C(14)−N(11)	1.324(7)
Ni(1)−N(3)	1.841(4)	N(2)−N(3)	1.365(7)	Ni(1)−N(4)	1.850(4)	N(4)−N(5)	1.396(7)
Ni(2)−N(7)	1.858(5)	N(8)−N(9)	1.359(6)	Ni(2)−N(12)	1.842(4)	N(11)−N(10)	1.382(6)
Ni(2)−N(9)	1.847(4)	N(3)−C(2)	1.350(7)	Ni(2)−N(10)	1.855(4)	N(4)−C(4)	1.317(7)
C(9)−S(1)	1.777(9)	N(9)−C(11)	1.342(7)	C(6)−S(2)	1.778(8)	N(10)−C(13)	1.316(6)
C(18)−S(3)	1.78(1)	C(2)−C(8)	1.494(8)	C(15)−S(4)	1.790(7)	C(4)−C(7)	1.510(9)
S(1)−C(1)	1.750(6)	C(11)−C(17)	1.505(8)	S(2)−C(5)	1.745(6)	C(13)−C(16)	1.503(8)
S(3)−C(10)	1.743(5)	C(2)−C(3)	1.398(8)	S(4)−C(14)	1.755(5)	C(4)−C(3)	1.436(7)
N(1)−C(1)	1.302(8)	C(11)−C(12)	1.416(7)	N(6)−C(5)	1.311(9)	C(13)−C(12)	1.420(7)
N(7)−C(10)	1.311(7)	C(3)−C(12)	1.504(7)	N(12)−C(14)	1.326(7)		
C(1)−N(2)	1.351(8)	S(1)···S(1′	3.627	C(5)−N(5)	1.342(8)	S(4)···S(3)	3.889

N(1)−Ni(1)−N(3)	83.0(2)	S(2)−C(5)−N(5)	120.6(5)	N(9)−Ni(2)−N(10)	95.1(2)	S(4)−C(14)−N(11)	118.6(4)
N(3)−Ni(1)−N(4)	96.2(2)	N(2)−N(3)−C(2)	116.1(4)	N(10)−Ni(2)−N(12)	83.4(2)	N(8)−N(9)−C(11)	115.9(4)
N(4)−Ni(1)−N(6)	82.8(2)	N(5)−N(4)−C(4)	116.9(5)	N(7)−Ni(2)−N(12)	97.9(2)	N(11)−N(10)−C(13)	116.6(4)
N(1)−Ni(1)−N(6)	98.0(3)	N(2)−N(3)−Ni(1)	116.2(3)	C(10)−N(7)−Ni(2)	111.4(4)	N(8)−N(9)−Ni(2)	116.1(3)
C(1)−N(1)−Ni(1)	111.9(4)	N(5)−N(4)−Ni(1)	116.2(3)	N(7)−Ni(2)−N(10)	174.9(2)	N(11)−N(10)−Ni(2)	115.1(3)
N(1)−Ni(1)−N(4)	178.4(2)	N(3)−C(2)−C(8)	118.0(5)	N(9)−Ni(2)−N(12)	175.0(2)	N(9)−C(11)−C(17)	117.4(5)
N(3)−Ni(1)−N(6)	177.2(2)	N(4)−C(4)−C(7)	118.7(5)	C(14)−N(12)−Ni(2)	111.5(4)	N(10)−C(13)−C(16)	118.2(5)
C(5)−N(6)−Ni(1)	113.1(4)	N(3)−C(2)−C(3)	120.5(5)	C(10)−N(8)−N(9)	108.9(4)	N(9)−C(11)−C(12)	120.8(5)
C(1)−N(2)−N(3)	108.4(5)	N(4)−C(4)−C(3)	121.4(5)	C(14)−N(11)−N(10)	108.9(4)	N(10)−C(13)−C(12)	121.5(4)
C(5)−N(5)−N(4)	107.1(5)	C(8)−C(2)−C(3)	121.5(5)	C(10)−S(3)−C(18)	101.2(4)	C(17)−C(11)−C(12)	121.8(5)
C(1)−S(1)−C(9)	103.3(4)	C(7)−C(4)−C(3)	119.8(5)	C(14)−S(4)−C(15)	102.2(3)	C(16)−C(13)−C(12)	120.2(4)
C(5)−S(2)−C(6)	104.4(3)	C(2)−C(3)−C(4)	126.8(5)	N(7)−C(10)−S(3)	127.4(4)	C(11)−C(12)−C(13)	126.4(5)
N(1)−C(1)−S(1)	127.1(5)	C(2)−N(3)−Ni(1)	127.5(4)	N(12)−C(14)−S(4)	120.4(4)	C(11)−N(9)−Ni(2)	128.0(4)
N(6)−C(5)−S(2)	118.5(5)	C(4)−N(4)−Ni(1)	127.0(4)	N(7)−C(10)−N(8)	120.5(5)	C(13)−N(10)−Ni(2)	128.1(3)
N(1)−C(1)−N(2)	120.4(6)	C(2)−C(3)−C(12)	118.0(5)	N(12)−C(14)−N(11)	121.0(5)	C(11)−C(12)−C(3)	115.2(4)
N(6)−C(5)−N(5)	120.8(6)	C(4)−C(3)−C(12)	115.0(5)	S(3)−C(10)−N(8)	112.1(4)	C(13)−C(12)−C(3)	118.2(4)
S(1)−C(1)−N(2)	112.5(4)	N(7)−Ni(2)−N(9)	83.2(2)				

Molecule **3B**

Ni(3)−N(13)	1.854(5)	C(28)−N(20)	1.41(1)	Ni(3)−N(18)	1.847(6)	C(23)−N(17)	1.335(9)
Ni(3)−N(15)	1.842(5)	N(14)−N(15)	1.375(7)	Ni(3)−N(16)	1.835(5)	C(32)−N(23)	1.34(1)
Ni(4)−N(19)	1.799(8)	N(20)−N(21)	1.399(9)	Ni(4)−N(24)	1.835(8)	N(17)−N(16)	1.377(7)
Ni(4)−N(21)	1.815(7)	N(15)−C(20)	1.333(7)	Ni(4)−N(22)	1.827(5)	N(23)−N(22)	1.387(8)
C(27)−S(5)	1.784(9)	N(21)−C(29)	1.345(9)	C(24)−S(6)	1.72(1)	N(16)−C(22)	1.337(7)
C(36)−S(7)	1.41(2)	C(20)−C(26)	1.504(9)	C(33)−S(8)	1.64(2)	N(22)−C(31)	1.334(8)
S(5)−C(19)	1.757(7)	C(29)−C(35)	1.49(1)	S(6)−C(23)	1.756(7)	C(22)−C(25)	1.509(8)
S(7)−C(28)	1.787(7)	C(20)−C(21)	1.432(8)	S(8)−C(32)	1.772(9)	C(31)−C(34)	1.508(8)
N(13)−C(19)	1.300(8)	C(29)−C(30)	1.422(8)	N(18)−C(23)	1.318(9)	C(22)−C(21)	1.420(8)
N(19)−C(28)	1.24(1)	C(21)−C(30)	1.492(8)	N(24)−C(32)	1.29(1)	C(31)−C(30)	1.416(8)
C(19)−N(14)	1.343(8)						

N(13)−Ni(3)−N(15)	83.6(2)	S(6)−C(23)−N(17)	118.4(5)	N(21)−Ni(4)−N(22)	95.3(2)	S(8)−C(32)−N(23)	118.2(8)
N(15)−Ni(3)−N(16)	95.6(2)	N(14)−N(15)−C(20)	116.4(5)	N(22)−Ni(4)−N(24)	84.9(3)	N(20)−N(21)−C(29)	116.9(7)
N(16)−Ni(3)−N(18)	83.6(2)	N(17)−N(16)−C(22)	116.0(5)	N(19)−Ni(4)−N(24)	92.3(4)	N(23)−N(22)−C(31)	116.3(5)
N(13)−Ni(3)−N(18)	97.1(2)	N(14)−N(15)−Ni(3)	115.4(3)	C(28)−N(19)−Ni(4)	108.0(6)	N(20)−N(21)−Ni(4)	114.6(5)
C(19)−N(13)−Ni(3)	111.0(4)	N(17)−N(16)−Ni(3)	116.0(4)	N(19)−Ni(4)−N(22)	175.9(3)	N(23)−N(22)−Ni(4)	114.7(4)
N(13)−Ni(3)−N(16)	178.4(2)	N(15)−C(20)−C(26)	118.1(5)	N(21)−Ni(4)−N(24)	177.4(3)	N(21)−C(29)−C(35)	117.6(6)
N(15)−Ni(3)−N(18)	178.6(2)	N(16)−C(22)−C(25)	117.7(5)	C(32)−N(24)−Ni(4)	109.7(6)	N(22)−C(31)−C(34)	117.2(5)
C(23)−N(18)−Ni(3)	110.9(4)	N(15)−C(20)−C(21)	120.9(5)	C(28)−N(20)−N(21)	102.8(7)	N(21)−C(29)−C(30)	121.0(6)
C(19)−N(14)−N(15)	108.4(5)	N(16)−C(22)−C(21)	121.4(5)	C(32)−N(23)−N(22)	107.2(6)	N(22)−C(31)−C(30)	121.0(5)
C(23)−N(17)−N(16)	108.1(5)	C(26)−C(20)−C(21)	120.9(5)	C(28)−S(7)−C(36)	95.0(9)	C(35)−C(29)−C(30)	121.4(6)
C(19)−S(5)−C(27)	102.9(4)	C(25)−C(22)−C(21)	120.9(5)	C(32)−S(8)−C(33)	101.2(6)	C(34)−C(31)−C(30)	121.7(5)
C(23)−S(6)−C(24)	102.0(7)	C(20)−C(21)−C(22)	125.7(5)	N(19)−C(28)−S(7)	117.2(6)	C(29)−C(30)−C(31)	125.2(5)
N(13)−C(19)−S(5)	126.4(5)	C(20)−N(15)−Ni(3)	128.2(4)	N(24)−C(32)−S(8)	118.3(7)	C(29)−N(21)−Ni(4)	128.5(5)
N(18)−C(23)−S(6)	120.2(5)	C(22)−N(16)−Ni(3)	128.0(4)	N(19)−C(28)−N(20)	127.3(7)	C(31)−N(22)−Ni(4)	128.8(4)
N(13)−C(19)−N(14)	121.5(6)	C(20)−C(21)−C(30)	118.5(5)	N(24)−C(32)−N(23)	123.4(8)	C(31)−C(30)−C(21)	117.9(5)
N(18)−C(23)−N(17)	121.3(6)	C(22)−C(21)−C(30)	115.8(5)	S(7)−C(28)−N(20)	115.5(6)	C(29)−C(30)−C(21)	116.6(5)
S(5)−C(19)−N(14)	112.1(4)	N(19)−Ni(4)−N(21)	87.4(4)				

in such an interaction. The next nearest intermolecular Ni ion from Ni3 is 7.620 Å away. This is schematically shown in Figure 4a.

Molecule **3A** also forms such a pair of dimers via a relatively short Ni2···Ni2a interaction at 3.220(2) Å. These tetranuclear units are then packed in such a fashion that the planes of Ni1 and Ni1a ae stacked via a significantly weaker Ni1··Ni1a contact at 3.617 Å. This results in an infinite chain of pairs of dimers. This is shown in Figure 4b. Note that the mean distance between the strong and weak Ni···Ni interaction of **3A** is 3.418 Å, which is very close to the value observed for the Ni4··· Ni4a contact in the isolated pair of dimers of **3B**. These Ni··· Ni contacts are reminiscent of those reported in solid bis-(dimethylglyoximato)nickel(II)[14] with a Ni···Ni distance at 3.250(5) Å and its partially oxidized forms $Ni(bqd)_2I_{0.018}$ with Ni···Ni contacts at 3.180(2) Å.[15,16] These attractive forces in the face-to-face dimers are considered to involve both metal−metal σ and δ bonding as well as ligand−ligand π bonding.[15]

(14) Godycki, L. E.; Rundle, R. E. *Acta Crystallogr*. **1953**, *6*, 487.
(15) (a) Brown, L. D.; Kalina, D. W.; McClure, M. S.; Schultz, S.; Ruby, S. L.; Ibers, J. A.; Kannewurf, C. R.; Marks, T. J. *J. Am. Chem. Soc*. **1979**, *101*, 2937. (b) Cowie, M.; Gleizes, A.; Grynkewich, G. W.; Kalina, D. W.; McClure, M. S.; Scaringe, R. P.; Teitelbaum, R. C.; Ruby, S. L.; Ibers, J. A.; Cannewurf, C. R.; Marks, T. J. *J. Am. Chem. Soc*. **1979**, *101*, 2921.
(16) Endres, H.; Keller, H. J.; Moroni, W.; Weiss, J. *Acta Crystallogr*. **1975**, *B31*, 2357.

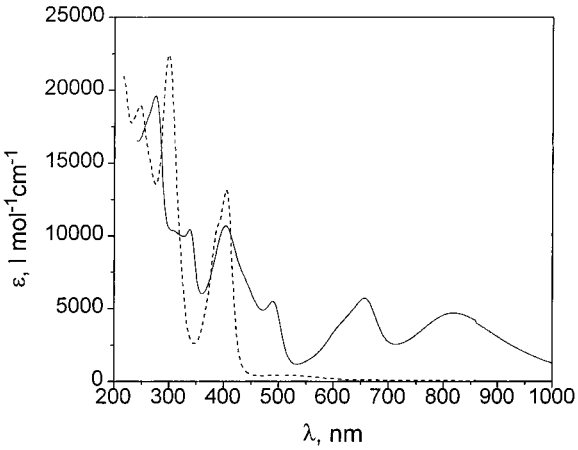

Figure 2. Electronic spectra of **3** in $CHCl_3$ and **4** in CH_3OH.

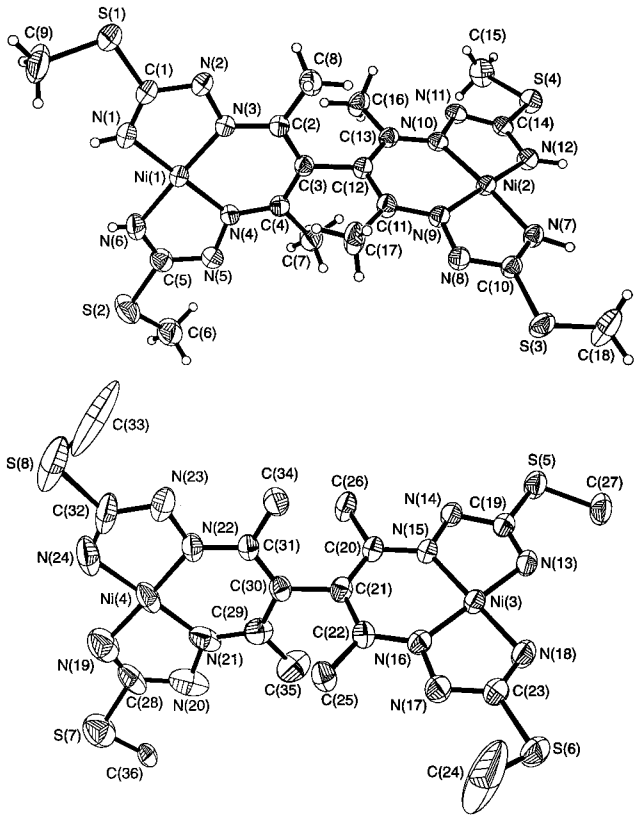

Figure 3. Structure of the neutral molecules **3A** (top) and **3B** (bottom) in crystals of **3**.

Magnetic Properties of Complexes. The molar magnetic susceptibility of solid samples of complexes **3** and **7** has been measured in the temperature range 2−300 K by using a SQUID magnetometer. Panels a and b of Figure 5 show the temperature dependence of the effective magnetic moment μ_{eff}, μ_B per dinuclear molecule of **3** and **7**, respectively. Values of μ_{eff} for solid **3** decrease with decreasing temperature from 0.7 μ_B at 300 K to a plateau value of 0.21 μ_B at 100 K. This behavior indicates some degree of antiferromagnetic coupling in solid **3**. Similar behavior but with quite different values of μ_{eff} has been observed for **7**. Here μ_{eff} also decreases with decreasing temperature from 1.35 μ_B at 300 K to 0.3 μ_B at 5 K. We take this result as a clear indication that the magnetic properties of solid **3** and **7** are predominantly determined by intermolecular interactions in the solid state which lead to effective diamagnetism in **3** most probably via the Ni···Ni contacts. In **7** the sterically more demanding *S*-dodecyl groups enforce a different packing, and consequently, the intermolecular contacts are

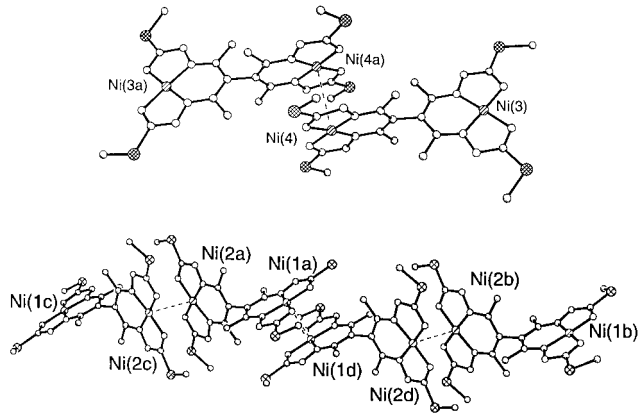

Figure 4. (a, top) Schematic representation of a pair of dimers **3B** in crystals of **3**; (b, bottom) schematic representation of an infinite chain of dimers **3A** in crystals of **3**.

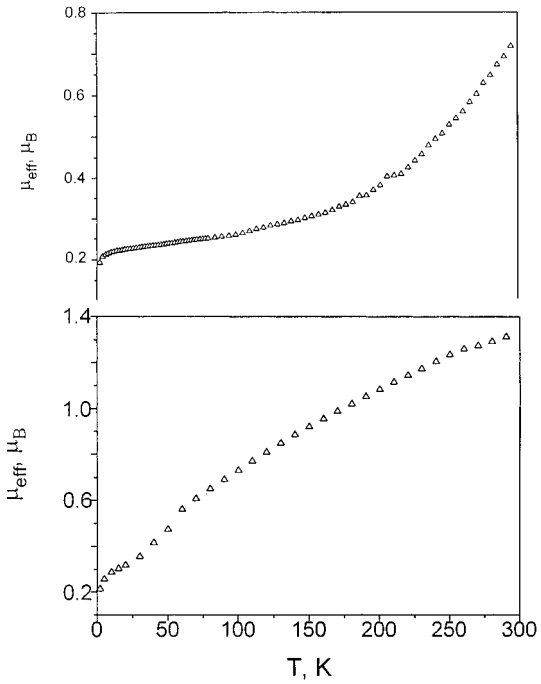

Figure 5. (a, top) Temperature dependence of the magnetic moment, μ_{eff}, per dinuclear unit of solid **3**; (b, bottom) temperature dependence of the magnetic moment, μ_{eff}, per dinuclear unit of solid **7**.

different from those in **3**. We have also measured the effective magnetic moment of **3** in $CHCl_3$ solution (0.56×10^{-2} M) by using the NMR method of Evans[17] in the temperature range 233−300 K. A temperature- and concentration-independent (0.54×10^{-2}−1.67×10^{-2} M) magnetic moment of 1.94 ± 0.06 μ_B per dinuclear unit has been determined. This solution value is significantly larger than in the solid state and clearly points to intermolecular coupling effects in the crystals. On the other hand, a magnetic moment of 2.45 μ_B is expected ($\mu_{eff} = (\mu_1^2 + \mu_2^2)^{1/2}$, $\mu_1 = \mu_2 = {}^1/_2$) for two uncoupled low-spin Ni(III) ions in a molecule of **3**. This is clearly not observed.

Complexes **1**, **2**, **4**, **5**, and **6** are diamagnetic both in the solid state and in solution (^{1}H NMR).

^{13}C CP/MAS NMR Spectra of 1−4. ^{13}C CP/MAS NMR spectra data of **1**−**4** are summarized in Table 4. All expected signals have been observed for **1**. It should be noted that the ^{13}C NMR spectra both in solution and in the solid state are quite similar. The only observed significant difference is the splitting

(17) (a) Evans, D. F. *J. Chem. Soc.* **1959**, 2003. (b) Sur, S. K. *J. Magn. Reson.* **1989**, *82*, 169.

Table 4. Chemical Shifts for **1**−**4** in 75 MHz ^{13}C NMR CP/MAS Spectra at 297 K[a]

compd	C1	C2	C3	C4	C5	solvent
1	158.5	147.2	92.8	24.0 (2)[b]	15.5 (1)	
					14.9 (1)	
2	161.0 (1)	146.0 (1)	95.0 (1)	24.1 (1)	14.1 (1)	57.3[c], 58.7[d]
	156.3 (1)	142.1 (1)		21.3 (1)	13.1 (1)	17.9; 21.1
3	179.2	117.0	80.1	36.3 (2)	17.9 (2)	
				32.9 (2)	14.7 (1)	
					11.7 (1)	
3[e]	167.5	145.1	78.5	19.8 (2)	17.5 (2)	
		141.6		19.0 (1)	15.4 (1)	
		127.4		18.6 (1)	13.8 (1)	
4	159.1	147.8	102.7	17.5	15.9	57.8[c]
						17.6

[a] Atom labels are as in Figure 8. [b] Relative intensities of signals are indicated in parentheses. [c] Fluxional. [d] Nonfluxional. [e] At $T = 85$ K.

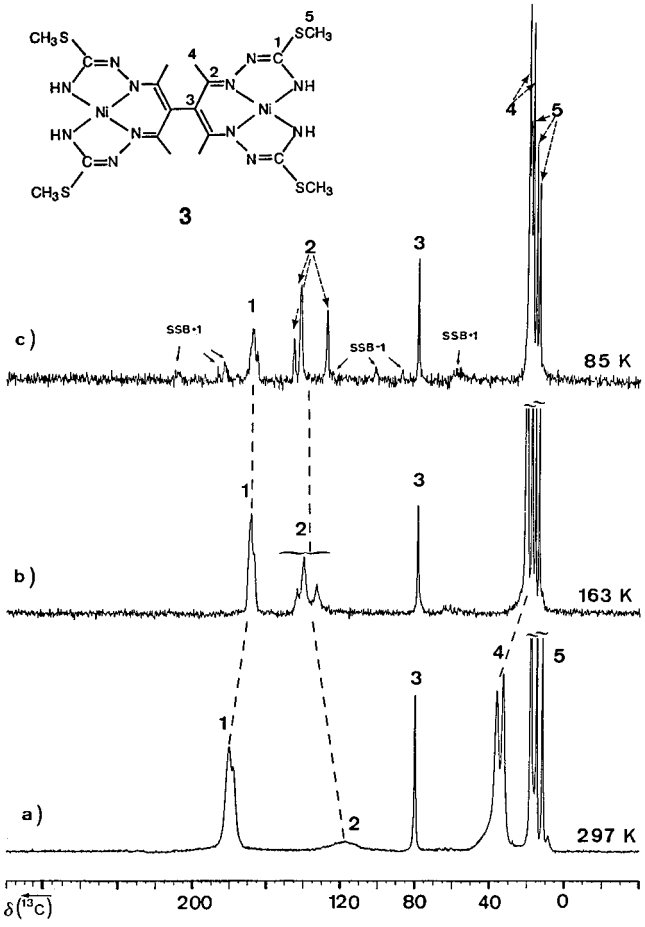

Figure 6. ^{13}C NMR CP/MAS spectra of **3** at variable temperature: (a, b) TOSS spectra; (c) spectrum without side band suppression. SSB, spinning side bands: +1 the first one to the higher frequency; −1 the first one to the lower frequency.

of SCH_3 signals in the solid state, which is probably due to the asymmetric intermolecular NI···I and S···S interactions in the solid state.

The ^{13}C CP/MAS NMR spectrum of **2** is fully consistent with C_1 symmetry in the solid state. The carbon atoms C1, C2, C4, and C5 (for atom labels see Figure 6) each display only one resonance in the solution ^{13}C NMR spectrum but show in the solid state two well-resolved lines of equal intensity for C1, C2, C4, and C6, and C1′, C2′, C4′, and C5′, respectively. This is in agreement with the chemical nonequivalence of the isothiosemicarbazide arms in **2**.

Figure 6 displays the solid state ^{13}C CP/MAS NMR spectra of **3** at three different temperatures. Temperature dependence

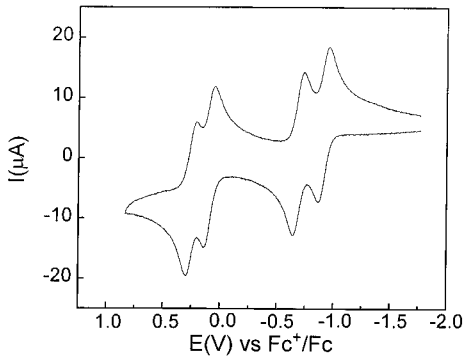

Figure 7. Cyclic voltammogram of **3** in CH_2Cl_2 (0.10 M [N(n-but)$_4$]-PF_6: glassy carbon working electrode; scan rate 200 mV/s.

of some resonances (chemical shift and line width) in the spectra of **3** is clearly observed. This is typical for contact shift effects. The most pronounced changes of the line shape and chemical shift are observed for the signals of the carbon atoms C1, C2, and C4, which indicates that they are in close proximity to the radical center of the molecule. High-field (for C1 and C4) and low-field (for C2) shifts are characteristic for positive or negative values of the hyperfine coupling constants. The solid state NMR spectra of **3** are in excellent agreement with the temperature-dependent magnetic measurements, indicating the noninnocence of the ligand system.

In the case of **4**, a total of seven resonances are observed both in solution and in the solid state ^{13}C NMR spectra, indicating the C_i symmetry of the dication. The small differences in chemical shifts of signals displayed in the solid state and solution NMR spectra are indicative of the lack of significant intermolecular bonding in the solid state. This is in agreement with the fluxionality of the solvent molecule, which is found in the ^{13}C CP/MAS NMR spectrum of **4** (see Table 4).

Electrochemistry. The electrochemical properties of complexes **3** and **7** have been studied by cyclic (CV) and square-wave voltammetry as well as coulometry. Cyclic and square-wave voltammograms in acetonitrile and/or dichloromethane solutions containing 0.10 M tetra-*n*-butylammonium hexafluorophosphate as supporting electrolyte and $\sim 10^{-3}$ M complex were recorded at scan rates ranging from 50 to 600 mV/s. The CV's of **3** and **7** in dichloromethane are very similar; they display four reversible 1 electron transfer waves at $E_{1/2} = -0.91$, -0.68, 0.10, 0.26 and -0.94, -0.71, 0.08, and 0.28 V vs the ferrocenium/ferrocene couple (Fc^+/Fc), respectively. Figure 7 shows the CV of **3**. In contrast, the CV of **3** in acetonitrile shows two reversible 1 electron transfer waves at $E_{1/2} = -0.83$ and -0.57 V and *one* reversible 2 electron wave at $E_{1/2} = 0.16$ V vs Fc^+/Fc. Coulometric reduction at -1.1 V vs Fc^+/Fc resulted in the passage of an average of 2.08 F (94555 C) of charge per mole of complex. Thus **3** and **7** are successively reduced by 2 electrons at negative potentials, whereas at positive potentials a 2 electron oxidation is observed, respectively.

The fully reduced form of **3** (and **7**) corresponds to the doubly deprotonated form of **5**: $[Ni^{II}(L^1-L^1)Ni^{II}]^{2-}$ (and $[Ni^{II}(L^2-L^2)$-$Ni^{II}]^{2-}$). We can then formulate four 1 electron oxidation steps which, in principle, may be metal- or ligand-centered as in

$$[Ni^{II}(L^1-L^1)Ni^{II}]^{2-} \underset{+e}{\overset{-e}{\rightleftharpoons}} [Ni^{II}(L^1-L^1)Ni^{III}]^{-} \underset{+e}{\overset{-e}{\rightleftharpoons}} [Ni^{III}(L^1-L^1)Ni^{III}] \underset{+e}{\overset{-e}{\rightleftharpoons}} [Ni^{III}(L^1-L^1)Ni^{IV}]^{+} \underset{+e}{\overset{-e}{\rightleftharpoons}} [Ni^{IV}(L^1-L^1)Ni^{IV}]^{2+} \quad (6)$$

3

or alternatively

$$[Ni^{II}(L^1{-}L^1)Ni^{II}]^{2-} \underset{+e}{\overset{-e}{\rightleftharpoons}} [Ni^{II}(L^{\bullet 1}{-}L^1)Ni^{II}]^{-} \underset{+e}{\overset{-e}{\rightleftharpoons}} [Ni^{II}(L^{\bullet 1}{-}L^{\bullet 1})Ni^{II}] \underset{+e}{\overset{-e}{\rightleftharpoons}} [Ni^{II}(L^1{-}L^{\bullet 1})Ni^{II}]^{+} \underset{+e}{\overset{-e}{\rightleftharpoons}} [Ni^{II}(L^1{-}L^1)Ni^{II}]^{2+} \quad (6a)$$

3

where $(L^1{-}L^1)^{6-}$ represents two 14 π-electron systems connected by a C−C single bond and $(L^1{-}L^1)^{2-}$ would be its twice 2 electron oxidized form (two 12 π-electron systems) and $(L^{\bullet 1}{-}L^{\bullet 1})^{4-}$ is a biradical.

Discussion

Although the molecular structure of **3** has been unequivocally established by X-ray crystallography, its electronic structure and, in particular, its magnetic properties deserve some comments.

The resonance structures for the various protonated forms of pentane-2,4-dione bis(*S*-alkylisothiosemicarbazone) ligand shown in Scheme 1 imply that the sum of the two C−C, four C−N, and two N−N bond distances of the ligand perimeter should be slightly longer than in its 2 electron oxidized forms because the former has four double bonds whereas the latter has five. This is indeed the case, as an analysis of this length in various crystallographically characterized complexes shows. Thus, in complexes containing a central metal ion with a well-defined localized oxidation state and an L^{3-} ligand, this sum is 13.52 ± 0.02 Å whereas in a complex containing L^- as a ligand it is slightly shorter at 13.47 Å. The average distance in **3** is 13.567 Å, which points to a description of the ligand as hexanionic $(L^1{-}L^1)^{6-}$ and, consequently, two nickel(III) ions.

It is now difficult to reconcile this fully localized $[Ni^{III}(L^1{-}L^1)Ni^{III}]$ description with the solid state magnetic properties of **3**. A square-planar low-spin Ni^{III} ion would accomodate one unpaired electron in an d_{z^2} metal orbital ($S_{Ni} = {}^1/_2$). Since molecule **3B** is packed in infinite chains via intermolecular Ni···Ni contacts, intermolecular antiferromagnetic coupling yielding a diamagnetic ($S = 0$) ground state is conceivable. On the other hand, molecule **3A** is packed in pairs. Given the structure of this pair, the two farmost separated outer nickel ions (Ni1 and Ni1a in Figure 6) should each carry an uncoupled spin of ${}^1/_2$ provided that no intramolecular antiferromagnetic coupling between the two nickel(III) ions occurs. This is a reasonable assumption because (i) the two magnetic orbitals are d_{z^2} which do not overlap and (ii) the two equatorial ligand planes are nearly perpendicular relative to each other. In the solid state one would expect **3** to exhibit residual paramagnetism of two uncoupled electrons per eight nickel ions ($\mu_{eff} = 1.2\ \mu_B$), which is clearly not the case. Furthermore, the solution magnetic moment would be anticipated to be $(\mu_1{}^2 + \mu_2{}^2)^{1/2} = 2.46\ \mu_B$, which is also not in agreement with the experiment.

Formulation of the ligand in its symmetric **2** electron oxidized form as biradical $(L^{\bullet 1}{-}L^{\bullet 1})^{4-}$ requires both nickel ions to be divalent: $[Ni^{II}(^{\bullet}L^1{-}{}^{\bullet}L^1)Ni^{II}]$. This form of **3** could be diamagnetic ($S = 0$) in the solid state or in solution provided that the biradical $(L^{\bullet 1}{-}L^{\bullet 1})^{4-}$ has a singlet ground state, which is unlikely. There are of course many other resonance structures possible for **3**; e.g., $[Ni^{II}(L^1{-}L^{\bullet 1})Ni^{III}] \leftrightarrow [Ni^{II}(L^{\bullet 1}{-}L^1)Ni^{III}] \leftrightarrow [Ni^{III}(L^1{-}L^{\bullet 1})Ni^{II}] \leftrightarrow [Ni^{III}(L^{\bullet 1}{-}L^1)Ni^{II}]$. These structures encompass a coordinated, delocalized ligand radical with $S = {}^1/_2$, $(L^1{-}{}^{\bullet}L^1)^{5-}$ and a diamagnetic Ni^{II} and one paramagnetic Ni^{III} ($S = {}^1/_2$). We find these formulations very appealing because they can accommodate the fine structural features of solid **3** and its magnetic properties as well as its unusual electronic spectrum. In this formulation, **3** is a mixed-valent compound which gives rise to intervalence type intense absorption bands in the visible or near-infrared. The pair formation of **3B** molecules would then occur at the Ni^{III} ions forming a very weak Ni···Ni bond (Ni4 and Ni4a in Figure 4b). At the same time Ni3 and Ni3a would be diamagnetic nickel(II), which do not generate a Ni···Ni contact. The radical anion would be antiferromagnetically coupled to the Ni^{III} ion and the pair of dimers, **3B** and **3B**, would have an $S = 0$ ground state in the solid state at low temperatures. In solution at temperatures 233−300 K, the observed magnetic moment of 1.94 μ_B would result from the intramolecular, presumably antiferromagnetic, coupling between the ligand radical and the nickel(III) ion ($\mu_{eff} < 2.45\ \mu_B$) in separated dimers. In the infinite chain structure of solid **3**, pairs of dimers of molecules **3A** are connected via very weak Ni1···Ni1a contacts. This is taken as evidence that the farmost separated outer Ni1 ions of a pair also carry some spin density in accord with the resonance structures shown above. Admittedly, this model is speculative but it is consistent with the available data.

Acknowledgment. We thank the Fonds der Chemischen Industrie for financial support of this work and Dr. U. Knof for valuable discussions of many aspects of this work.

Supporting Information Available: Tables listing details of crystal structure determination of **3**, atom coordinates, calculated positional parameters for the hydrogen atoms, bond distances and angles, the square-wave voltammogram, and anisotropic thermal parameters of **7** (10 pages). Ordering information is given on any current masthead page.

IC960802O